Computer analysis of explosive sensitivity to projectile impact

Adam Wiśniewski

Military Institute of Armament Technology, 7 Prymasa Stefana Wyszyńskiego str., 05-220 Zielonka, PL

Abstract: The use of different ERA reactive cassettes is shown. Functioning rules of reactive one-(ERAWA-1) and two-layered (ERAWA-2) reactive cassettes are presented. Different kinds of tests with ERAWA armours are shown. There are some examples of the simulation of impact of different types AP and HEAT ammunition. Simulation was based on "free points" and AUTODYN2D &3D computer programs.

1. Characteristics of reactive armours

In continuous "competition" between armour and projectile, especially, shaped charge projectiles, during the last years essential progress has been noted. These projectiles [1] of $d = 70 \div 155$ mm calibre usually have copper liner, and angle of liner $\varphi = 40 \div 60°$, (Table 1).
Projectiles or mines, for example, explosively formed projectiles EFP of $d = 50 \div 200$ mm calibre and with large mass of explosive material are the greate threat for tanks [3] (Table 1).

Table 1. Parameters of shaped charge and explosively formed projectiles

Kind of projectile / energy of penetrator E	Mass of jet (m_J) / mass of cluster, (m_Z)		Length of jet / length of cluster, l_J / l_Z	Diameter of jet / diameter of cluster d_J / d_Z	Speed of jet / speed of cluster, V_J / V_Z	Distance between projectile and RHA, l	Diameters of entry / mouth crater d_1 / d_2,	Depth of penetration of RHA DP,
[MJ]	m_J [m]	m_Z [m]	[mm]	[mm]	[m s^{-1}]	[m]	[mm]	[mm]
HEAT / 1,5 ÷ 9	0,2	0,8	< 1500 / < 200	≤ 0,2 d / 0,2 d 5 ÷ 30 / ≤ 30	≤ 8500 / 1500 ÷ 2000	2 ÷ 10 d 0,14 ÷ 1,5	≤ 0,3 d / 0,1d 50 / 10	3 ÷ 8 d 300 ÷ 1300
EFP / 3 ÷ 10	0,8	0,2	0,1 d / d	0,1 d / 0,5 d 50 ÷ 100	≤ 1000 / ≤ 2500	10 ÷ 1000 d 1 ÷ 200	0,5 d / 0,49 d 50 ÷ 100 / 49 ÷ 90	0,6 ÷ 0,85 d 60 ÷ 170

ERA reactive armour (Fig. 1, 2) is even more efficient way of tank protection. It consists of cassettes in cuboid form, made of metal and filled with explosive material. These cassettes, placed at some distance of frontal plate and tank turret, are the screen in front of main armour. After perforation of cassette casing, shaped charge jet hits explosive material, causing its detonation. As a result there is a strong dispersion of part of shaped charge jet, which perforation ability decreases considerably after penetrating this cassette. In majority of hits it is sufficient to efficiently protect main armour of tank, which will not be penetrated then.
In Military Institute of Armament Technology in Zielonka three generations of reactive cassettes for tank PT-91 "Hard" [2-6] - ERAWA-1 and ERAWA-2 with module and block way of assembly were designed and next they were implemented in" Bumar-Łabędy" Plant and one of the examples of the third generation is presented in Figure 3.
In some foreign solutions distances between cassettes are very large (40 ÷ 50) mm (Fig. 1, 2), what ensures protection of (60 ÷ 70)% flat surface. ERAWA cassettes can contact each other, and due to that flat surface is covered in 95%.

Fig. 1. American tanks in Persian Gulf with reactive cassettes

Fig. 2. Ukrainian tank T-84 with reactive cassettes CONTACT

Fig. 3. Polish tank PT-91 Hard with quickly assembled blocks of ERAWA-1 and ERAWA-2 reactive cassettes (III generation)

Now a way of test of reactive armours will be shown on example of test of ERAWA-1 and ERAWA-2 cassettes, taking into account part of general requirements for such armours.

Very close placed above neighbouring cassettes require the use of explosive (in these cassettes) as:

a) very sensitive to react during impact of:
   - shaped charge jet (Fig. 4, 5),
   - APFSDS projectile (Fig. 6, Tab. 2),
   - EFP projectile (Fig. 7, 8).;

b) insensitive to react:
   - during impact of:
   - AP small calibre ammunition (Fig. 9, 10, Tab. 2),
   - fragments from exploded projectiles (Fig. 11, 12),
   - of neighbouring cassettes during the explosion of impacted cassette (Fig. 5),
   - during burning of:
     - petrol (Fig. 13, 14),
     - napalm (Fig. 15, 16),
     - thermite (Fig. 17, 18).

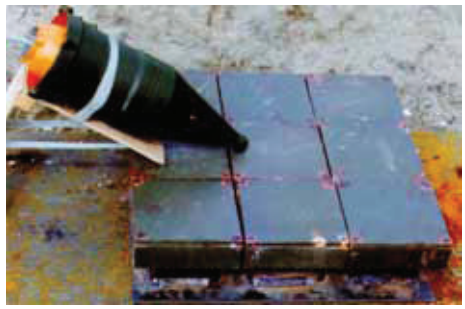

Fig. 4. Scheme of test of protective ability non-transferring detonation among ERAWA-2 block cassettes ($\infty = 60°$) with the use of 9M114M warhead (Malutka)

Fig. 5. Detonated ERAWA-1 cassette and destroyed neighbouring cassettes of block of nine cassettes, with 125 mm projectile BK-14M (HEAT, $\infty = 60°$). Penetration of RHA armour $h_w = 30$ mm, protective ability of cassette $CP = 94$ %

Fig. 6. Crater in plate of RHA armour after firing ERAWA-2 cassette from tank, with 125 mm projectile BM-15 (APFSDS-T, $h = 300$ mm, $\infty = 60°$). Penetration of RHA armour $h_w = 130$ mm, protective ability of cassette $CP = 57\%$

Fig. 7. Scheme of test of protective ability of ERAWA-2 cassette (2) by firing with the use of EFP warhead (1) (d = 100 mm, $h = 85$ mm), ($\infty = 60°$)

Fig. 8. Traces on RHA armour after penetration of ERAWA-2 cassette with warhead EFP; 1 - trace of detonation of ERAWA-2 cassette, 2 - trace of destroyed EFP projectile (EFP – $h = 85$ mm), $h_w = 5$ mm, protective ability of cassette $CP = 94$ %, ($\infty = 60°$)

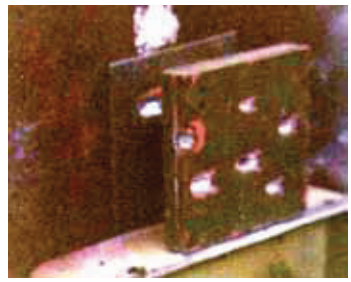

Fig. 9. ERAWA-1 cassette after firing with six 7.62 mm armour-piercing projectiles B-32 ($\infty = 60°$)

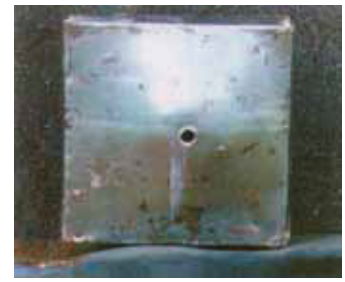

Fig. 10. ERAWA-1 cassette after firing with 12.7 mm armour-piercing projectiles B-32 ($\infty = 0$)

Fig. 11. Scheme of resistance test of ERAWA-1 cassettes to detonation and destruction with explosion of 82 mm mortar grenade

Fig. 12. ERAWA-1 cassettes after explosion of 82 mm mortar grenade

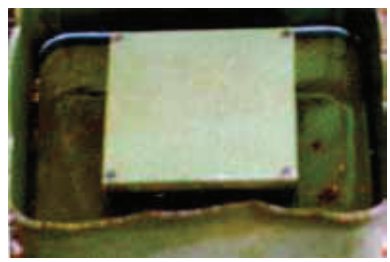

Fig. 13. Scheme of resistance test of ERAWA-1 cassette to detonation and destruction during burning of petrol around it

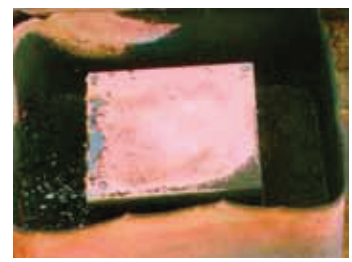

Fig. 14. ERAWA-1 cassette after combustion of petrol around it

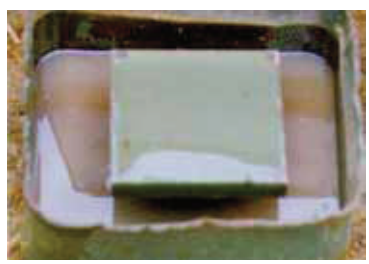

Fig. 15. Scheme of resistance test of ERAWA-1 cassette to detonation and destruction during burning of napalm on it and around it

Fig. 16. ERAWA-1 cassette after combustion of napalm on it and around it

Fig. 17. Scheme of resistance test of ERAWA-1 cassette to detonation and destruction during burning of incendiary bomb ZAB-2,5 containing thermite (3000 °C) on it

Fig. 18. ERAWA-1 cassette after combustion of incendiary bomb ZAB-2,5 on it

Table 1. Parameters of Polish KE projectiles

No	Cali-bre of projectile d [mm]	Kind of projectile	Mass of projectile m_p, ($m_{p\,m}$) [g]	Speed of projectile V_p, ($V_{p\,m}$) [m s^{-1}]	Average kinetic energy of projectile $E_{śr}$, [J]	Thickness of RHA plate and penetration depth (h) /distance (l), / angle (∞)			Comments, probability of penetration (p_p) and inflammation $\{p_z\}$, [%]
						h [mm]	l [m]	∞ [°]	
1	7.62	B-32	9.95	840 ÷ 855 (847.5)	3573	10	200	0	inflammation of container with petrol behind target at distance of L = 0.1÷0.4 m, (80), {---}
2	12.7	B-32	47.4 ÷ 49 (48.2)	810 ÷ 825 (817.5)	16106	20	200	0	(90), inflammation of container with petrol behind target ≠15, L = 70 m, {75}
3	14.5	BZT	59.3 ÷ 61.3 (60.3)	995 ÷ 1015 (1005)	30452	20	100	20	(80), inflammation of container with petrol behind target ≠20, L = 100 m, {80}
						(21.3)			
4	14.5	B-32	63 ÷ 64.8 (63.9)	980 ÷ 995 (987.5)	31156	20	100	20	(80), inflammation of container with petrol behind target ≠20, L = 100 m, {80}
						(21.3)			
5	125	APFS DS	4100	1650	5.58	550	100	0	---

2. Model of detonation process of phlegmatized hexogen

The propagation of the detonative wave in the explosive has been described with the use of the approximation of so-called "the detonative optics", in which the front of the detonative wave is a surface of the strong discontinuity, of the well-known shape (for the punctual initiation – the front is spherical), and the parameters of the medium on this surface are defined by the Chapman-Jouguet's point. Propagation of the detonation products and their influence on the liner of the RPG-7M projectile are described with the use of equations of the hydrodynamics for the cylindrical symmetry:

- Conservation law of hydrodynamic detonation theory in cylindrical geometry:

- Mass conservation law:

$$\frac{d\rho}{dt} + \rho \cdot \mathrm{div}\,\vec{w} = 0\,, \tag{1}$$

- Momentum conservation law:

$$\rho \frac{du}{dt} = -\frac{\partial p}{\partial r}\,, \tag{2}$$

$$\rho \frac{dv}{dt} = -\frac{\partial p}{\partial z}\,, \tag{3}$$

- Energy conservation law:

$$\rho \frac{dE}{dt} = -p \cdot \mathrm{div}\vec{w} + \rho Q \frac{d\alpha}{dt}\,, \tag{4}$$

$$\frac{d\alpha}{dt} = K \cdot \alpha^{\gamma} (1-\alpha)^{1-\gamma} p \cdot E\,, \tag{5}$$

where: α – burn-up factor ($\alpha = 0$ – non reacted material; $\alpha = 1$ - totally reacted material);

$$Q = Q_h(1-B), \tag{6};$$

B - mass fraction of phlegmatized hexogen; Q_h – heat of reaction ($Q_h = 5.5265 \cdot 10^{10}$ [erg g^{-1}]). K and γ are coefficients:

$$K = 0.48 \cdot 10^{-14}\left(1 + \frac{0.08}{1.75 - \rho_0}\right), \tag{7}$$

$$\gamma = 0.13\left(1 + \frac{0.2}{1.75 - \rho_0}\right), \tag{8}$$

where: ρ_0 - initial density of phlegmatized hexogen [g cm^{-3}].

- Total pressure:

$$p = \alpha \cdot p_{PD} + (1-\alpha) p_{MW}\,, \tag{9}$$

where: p_{PD} - pressure of detonation products; p_{MW} – pressure in non reacted material;

$$p_{PD} = A e^{-\frac{a}{\rho}}\left(1 - \rho S_1\right) + S_2 \rho^2 + \gamma_{PD} \rho E\,, \tag{10}$$

where: $A = 8.9616 \cdot 10^{12}$ [dyn cm^{-2}]; $a = 10.106$ [g cm^{-2}]; $\gamma_{PD} = 0.3$; $S_1 = 2.9685 \quad 10^{-2}$ [cm^3 g^{-1}]; $S_2 = 2.786 \quad 10^{10}$ [dyn·cm^4 g^{-2}], and:

$$p_{MW} = C\left(1 - x^3\right) + S\left(x^{\frac{2}{3}} - 1\right) x^{\frac{5}{3}} + \Gamma \rho E\,, \tag{11}$$

where: $x = \rho / \rho_k$; $\rho_k = 1.72$ [g cm^{-3}]; $\Gamma = 2.4$, $C = 7.12 \cdot 10^{10}$ [dyn cm^{-2}]; $S = 41.18 \cdot 10^{10}$ [dyn cm^{-2}].

- A. Equation of state of detonation products in the form of JWL

The system of equations was supplemented with the equation of state of detonation products in the form of JWL:

$$p_{PD} = A\left(1-\frac{\delta}{R_1 V}\right)^{-R_1 V} + B\left(1-\frac{\delta}{R_2 V}\right)^{-R_2 V} + \delta\rho\varepsilon\,, \tag{12}$$

where: $V = \rho_0 / \rho$; A, B, R_1, R_2, δ - empirical constants.

In case of lack of the knowledge of the shape of detonative wave front, more complicated model is used, in which the shape of the front results from the solution of equations of the motion of detonation products and of equations of chemical macrokinetics. The equation of conservation of energy has the form of [30]:

$$\rho\frac{dE}{dt} = -p \cdot \operatorname{div} \bar{w} - Q\frac{d\alpha}{dt}\,, \tag{13}$$

where: α - the coefficient of the burning; Q - heat of combustion of the explosive unit.
The equation of macrokinetics of chemical reactions was accepted in the form of the Arhenius's equation:

$$\frac{d\alpha}{dt} = -\nu\alpha \cdot \exp\left(-\frac{E_a}{RT}\right), \tag{14}$$

where: ν - the collision coefficient; E_a- the activation energy; R - the gas constant; or the Forest Fire's equation:

$$\frac{d\alpha}{dt} = -\alpha \cdot \exp\left(A + Bp + Cp^2 + \cdots + Xp^n\right). \tag{15}$$

Basic data can be found in very many sources, but there is little and often incomplete information concerning information such details as gap creation, the influence of gaps on strength properties, sticky effects, coefficients of the Forest Fire's equation.

- B. The jet of RPG-7 projectile + the reactive cassette (steel/ TNT / steel - 5/5/5/ mm)

Table 3. Coefficients in the JWL equation for explosives of RPG-7M projectile

Parameter	Phlegmatizated octogen	Phlegmatizated hexogen
ρ_0, [g cm^{-3}]	1.783	1.777
D, [m s^{-1}]	8730	8500
$p_{CJ,}$ [dyn cm^{-2}]	$3.35 \cdot 10^{11}$	$3.4 \cdot 10^{11}$
A, [dyn cm^{-2}]	$9.433 \cdot 10^{12}$	$6.347 \cdot 10^{12}$
B, [dyn cm^{-2}]	$8.805 \cdot 10^{10}$	$0.8 \cdot 10^{11}$
R_1	4.70	4.20
R_2	0.90	1.0
δ	0.35	0.3
$\rho_0\varepsilon_0$, [dyn cm^{-2}]	$1.02 \cdot 10^{11}$	$8.9 \cdot 10^{10}$

Table 4. Data of the copper RPG-7M liner - physical model - elastic-plastic body

No.	Parameter	Value
4	ρ_0 [g cm^{-3}]	8.93
5	γ_0	1.99
6	k_1 10^{12} [dyn cm^{-2}]	1.386
7	k_2 10^{12} [dyn cm^{-2}]	2.749
8	k_3 10^{12} [dyn cm^{-2}]	5.113
9	E_{00} 10^{9} [erg g^{-1}]	-1.178
10	E_{01} 10^{9} [erg g^{-1}]	-2.344
11	E_{02} 10^{10} [erg g^{-1}]	7.529

No.	Parameter	Value
12	E_{03} 10^{11} [erg g^{-1}]	1.526
13	E_{04} 10^{11} [erg g^{-1}]	2.19
14	Y_0 10^{9} [dyn cm^{-2}]	1.2
15	Y_{max} 10^{9} [dyn cm^{-2}]	6.0
16	μ_0 10^{11} [dyn cm^{-2}]	4.77
17	T_{m0} 10^{3} [K]	1.79
18	β	36.0
19	n	0.45

No.	Parameter	Value
20	b 10^{-12} [dyn cm^{-2}]	3.0
21	h 10^{-4} [K^{-1}]	3.8
22	k 10^{-2} [dyn cm^{-2} s^{-1}]	1.0
23	σ_0 10^{9} [dyn cm^{-2}]	7.0
24	V_{C0} 10^{-6} [cm^{3} g^{-1}]	1.27
25	V_{C1} 10^{-3} [cm^{3} g^{-1}]	3.0

Table 5. The explosive of the reactive cassette

Physical model Model „of detonative optics”	TNT material	Diameter 300 mm	Thickness 5 mm

Table 6. The model of the detonative optics (TNT)

Parameters in the point C - J			Coefficients of the JWL equation of state					
p_H	$\rho_0 \cdot E_0$	D	ρ_0	A	B	R_1	R_2	δ
10^{12} [dyn cm^{-2}]	10^{12} [dyn cm^{-2}]	[km s^{-1}]	[g cm^{-3}]	10^{12} [dyn cm^{-2}]	10^{12} [dyn cm^{-2}]	-	-	-
0.21	0.07	6.93	1.63	3.712	0.0323	4.15	0.95	0.3

Table 7. Data of steel reactive cassette for: 1 - Diameter of armour (d_p) = 300 [mm]; 2 - Thickness of armour (l_p) = 5 [mm]; Velocity of armour -, - physical model - elastic-plastic body

No.	Parameter	Value
4	ρ_0 [g cm^{-3}]	7.9
5	γ_0	2.17
6	k_1 10^{12} [dyn cm^{-2}]	1.6481
7	k_2 10^{12} [dyn cm^{-2}]	3.124
8	k_3 10^{12} [dyn cm^{-2}]	5.6491
9	E_{00} 10^{9} [erg g^{-1}]	-1.34
10	E_{01} 10^{9} [erg g^{-1}]	-2.908
11	E_{02} 10^{10} [erg g^{-1}]	1.012

No.	Parameter	Value
12	E_{03} 10^{11} [erg g^{-1}]	2.051
13	E_{04} 10^{11} [erg g^{-1}]	2.901
14	Y_0 10^{9} [dyn cm^{-2}]	4.4
15	Y_{max} 10^{9} [dyn cm^{-2}]	2.0
16	μ_0 10^{11} [dyn cm^{-2}]	7.7
17	T_{m0} 10^{3} [K]	1.93
18	β	40.0
19	n	0.35

No.	Parameter	Value
20	b 10^{-12} [dyn cm^{-2}]	3.0
21	h 10^{-4} [K^{-1}]	4.5
22	k 10^{-2} [dyn cm^{-2} s^{-1}]	2.5
23	σ_0 10^{9} [dyn cm^{-2}]	1.55
24	V_{C0} 10^{-6} [cm^{3} g^{-1}]	1.27
25	V_{C1} 10^{-3} [cm^{3} g^{-1}]	6.33

3. The results of simulation

The results of simulation process of impact AP ammunition of 7.62 mm, 12.7 mm 14.5 mm, and 125 mm calibre the type of APFSDS are presented in Figures 19÷22. In these figures the change of following parameters on the Z axis: density ρ, thickness L, collapsing velocity Vzg and pressure P during penetration of ERA in function t, are presented.

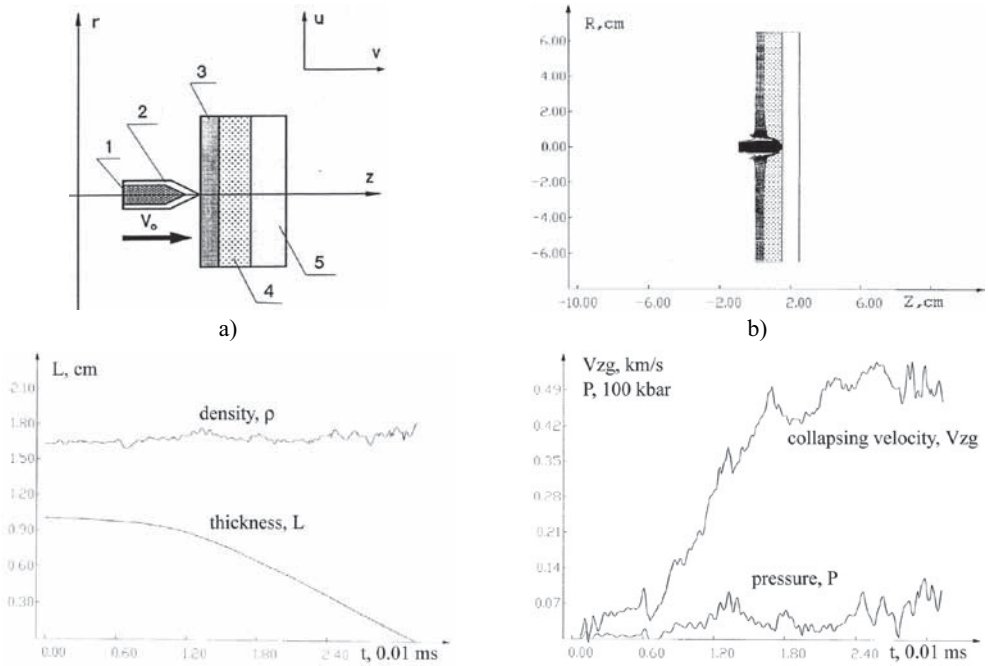

Fig. 19. Parameters of explosive while impact of 7.62 mm AP on ERA with velocity of v = 855 [m s^{-1}]: - a) scheme of experimental stand- 1 rod; 2 – coat; 3, 5 – steel; 4 – explosive; t = 0 [ms]; b) – for t = 0.032 [ms]

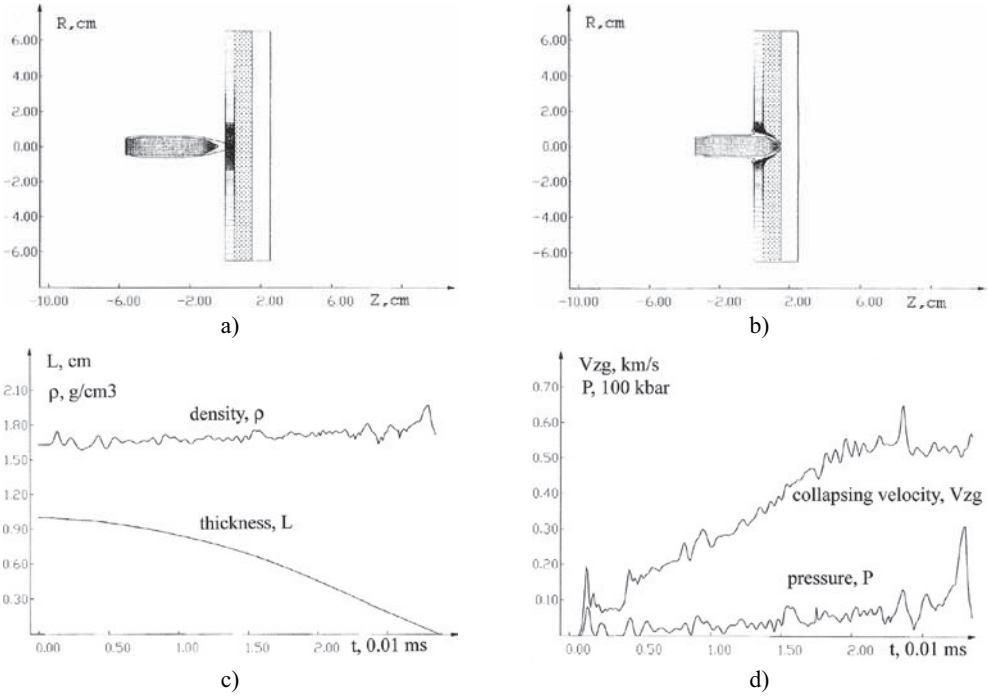

Fig. 20. Parameters of explosive while impact of 12.7 mm AP on ERA with velocity v = 820 m/s; a) - for t = 0 [ms]; b) – for t = 0.032 [ms]

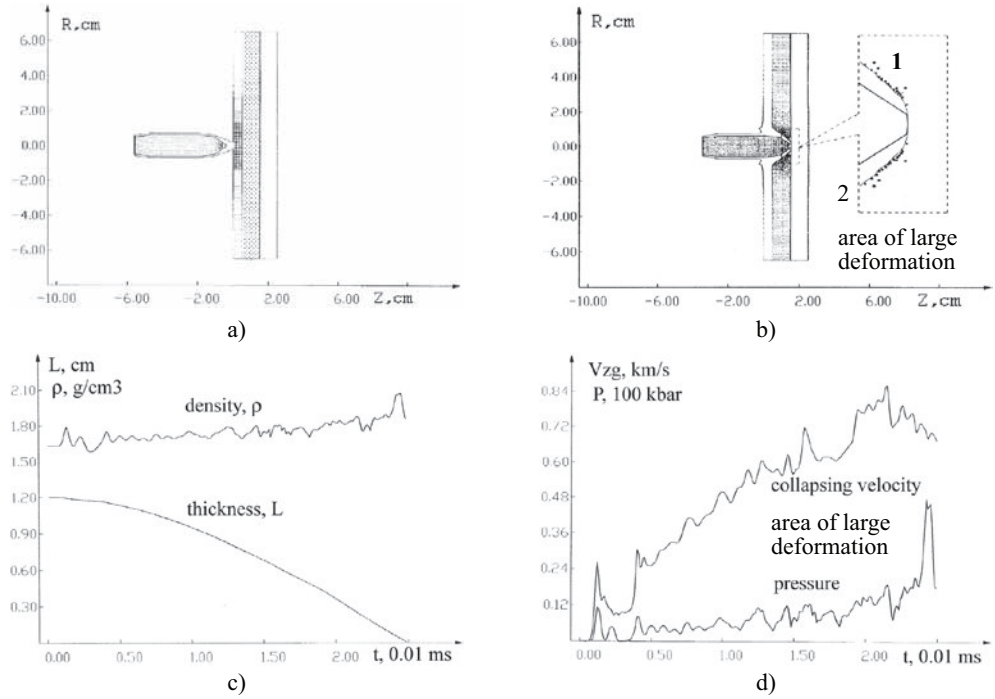

Fig. 21. Parameters of PBX 9404 explosive while impact of 14.5 mm AP on ERA with velocity v = 995 [m s^{-1}]: a) - for t = 0 [ms]; b) – for t = 0.023 [ms], 1 - non reacted explosive (F=0), 2 - detonation products (F=1)

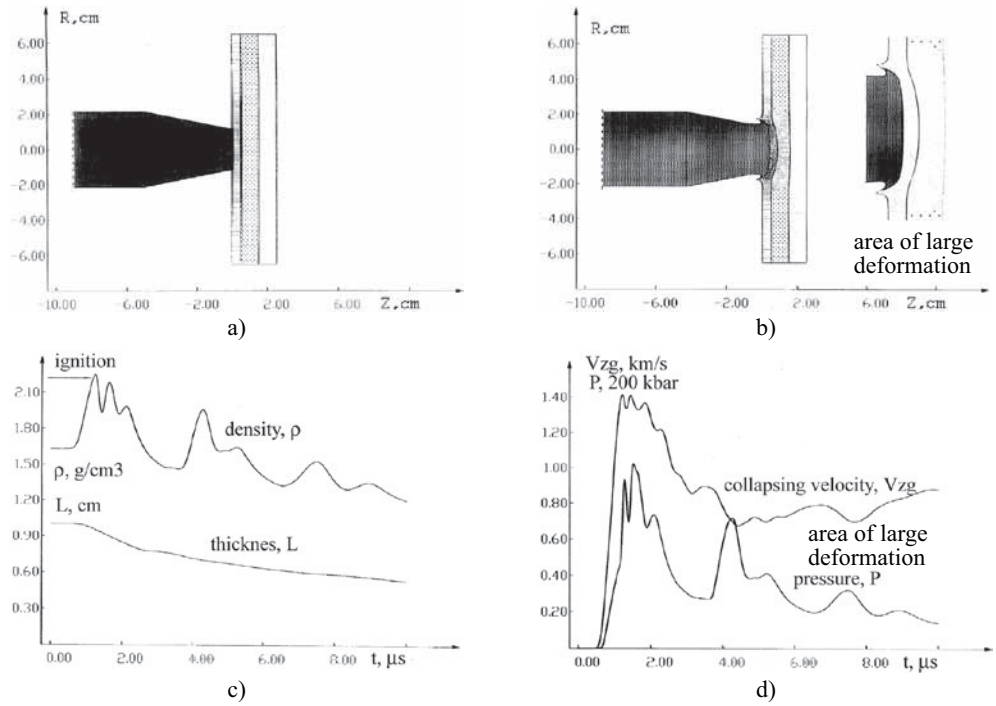

Fig. 22. Parameters of explosive while impact of 125 mm APFSDS on ERA with velocity v=1800 m/s: a) - for t = 0 [μs]; b) – for t = 4 [μs]

The next step to test the sensitivity of different types of ERA cassettes, containing different explosive layers placed on target, is the observation of their reaction to impact of KE (kinetic energy) ammunition. Explosive contains different percentages of phlegmatizing agent. The examples of reaction of two-layered explosive of different thickness (3 ÷ 15) mm with different contents of phlegmatizing agent (70 ÷ 97.4)%, are illustrated in Figures 23÷31.

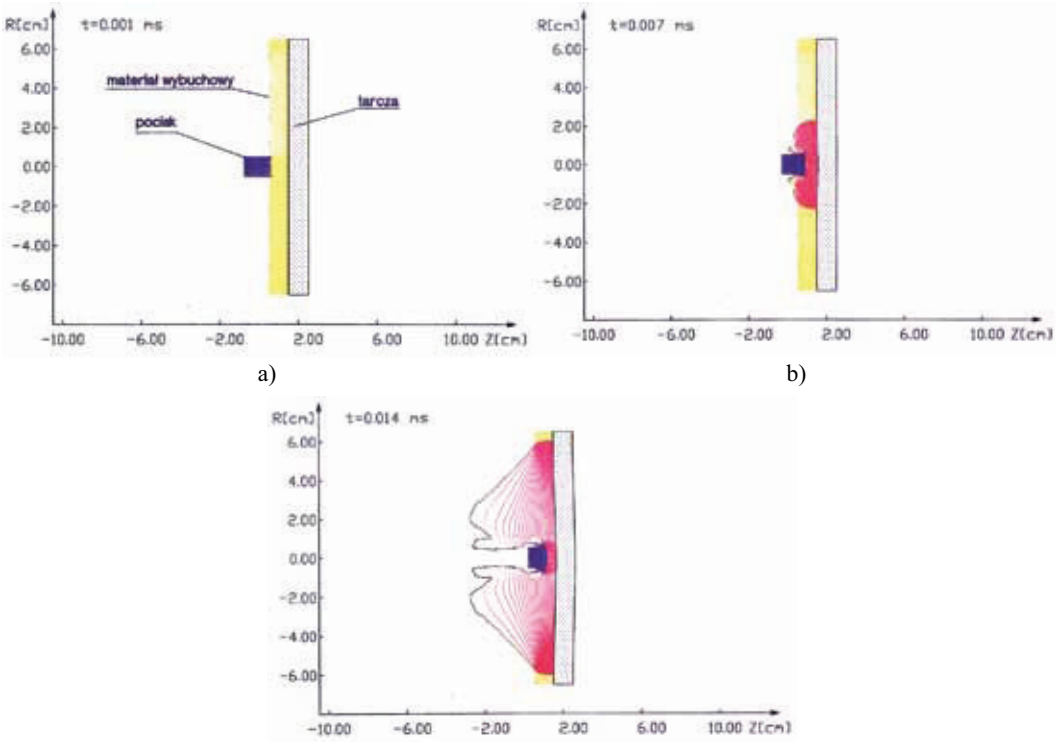

Fig. 23. Reaction of ERA cassette (of 10 mm thickness of explosive layer, containing 70% phlegmatizing agent) to impact of KE projectile with the speed of V_{AP} = 800 [m s^{-1}]

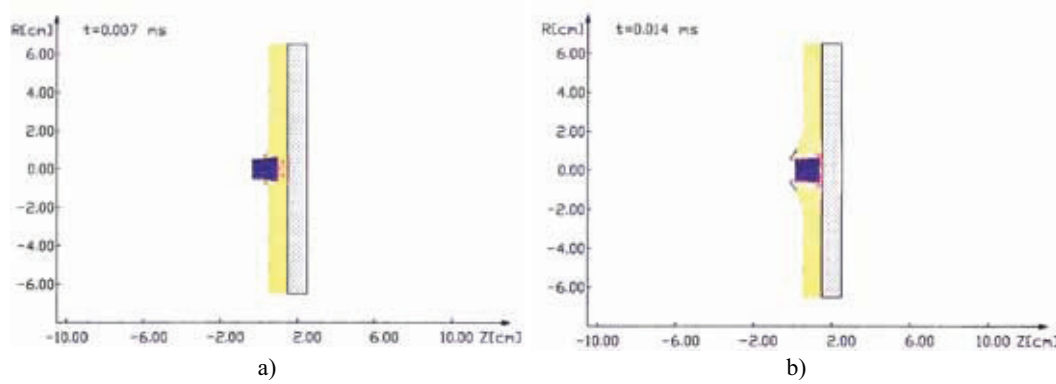

Fig. 24. Reaction of ERA cassette (of 10 mm thickness of explosive layer, containing 77.5% phlegmatizing agent) to impact of KE projectile with the speed of V_{AP} = 800 [m s^{-1}]

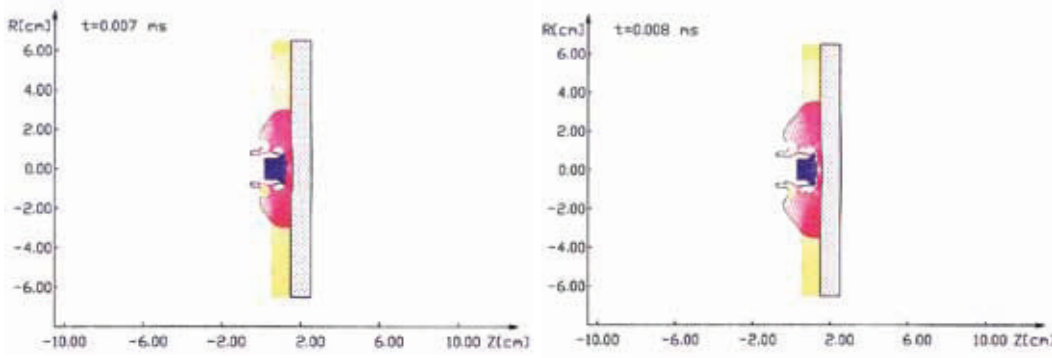

a) b)

Fig. 25. Reaction of ERA cassette (of 10 mm thickness explosive layer, containing 77.5% phlegmatizing agent) to impact of KE projectile with the speed of V_{AP} = 1600 [m s^{-1}]

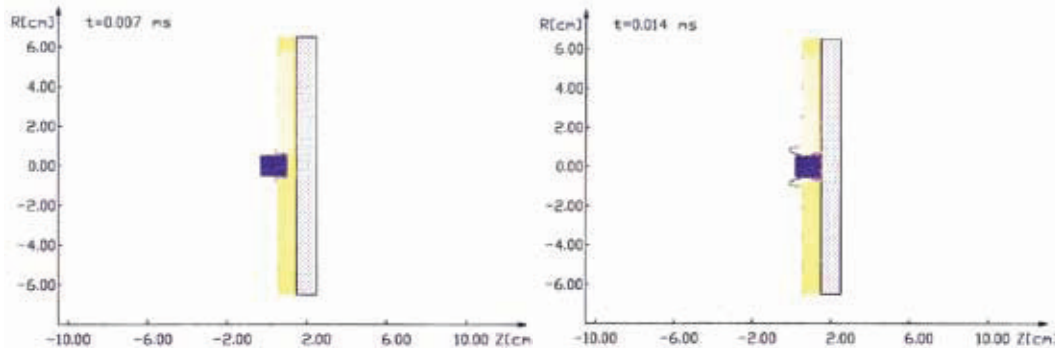

a) b)

Fig. 26. Reaction of ERA cassette (of 10 mm thickness explosive layer, containing 90% phlegmatizing agent) to impact of KE projectile with the speed of V_{AP} = 800 [m s^{-1}]

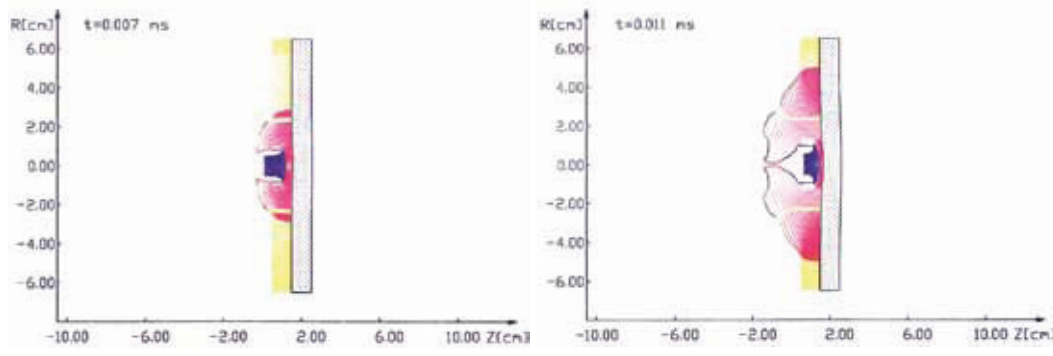

a) b)

Fig. 27. Reaction of ERA cassette: a) of 10 mm thickness explosive layer, containing 80% phlegmatizing agent; b) 3 mm thickness interlayer and internal radius 20 mm, to impact of KE projectile with the speed of V_{AP} = 1600 [m s^{-1}]

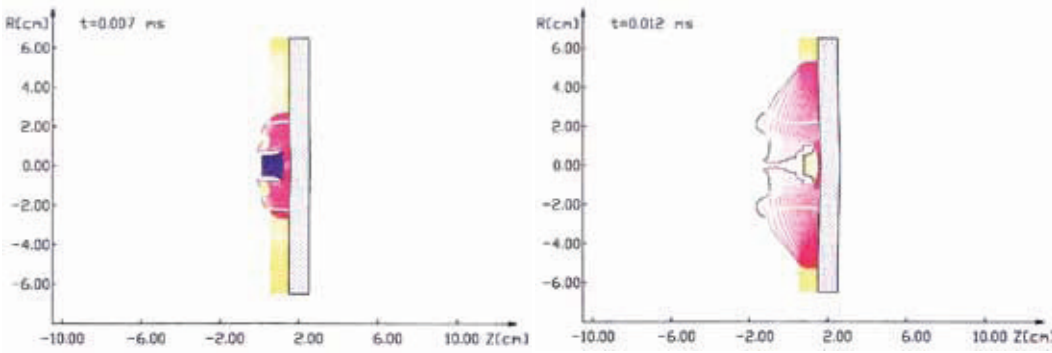

a) b)

Fig. 28. Reaction of ERA cassette: a) of 10 mm thickness explosive layer, containing 80% phlegmatizing agent; b) 15 mm thickness interlayer and internal radius 20 mm - 100% phlegmatizing agent, to impact of KE projectile with the speed of $V_{AP} = 1600$ [m s^{-1}]

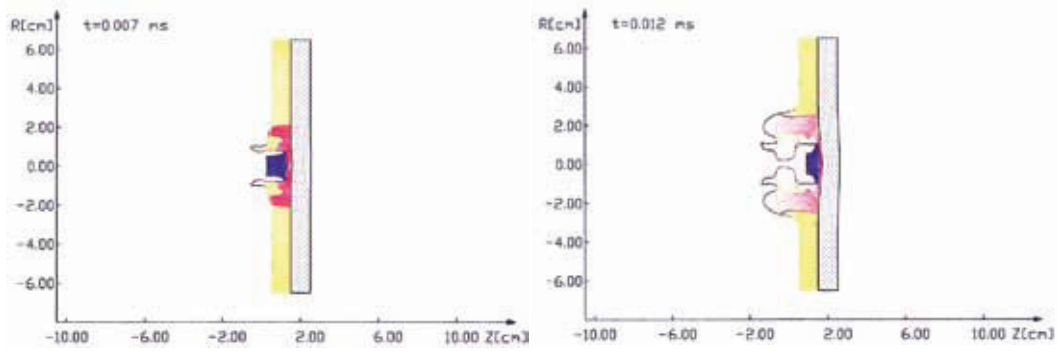

a) b)

Fig. 29. Reaction of ERA cassette: a) of 10 mm thickness explosive layer, containing 90% phlegmatizing agent; b) 10 mm thickness interlayer and internal radius 20 mm - 100% phlegmatizing agent, to impact of KE projectile with the speed of $V_{AP} = 1600$ [m s^{-1}]

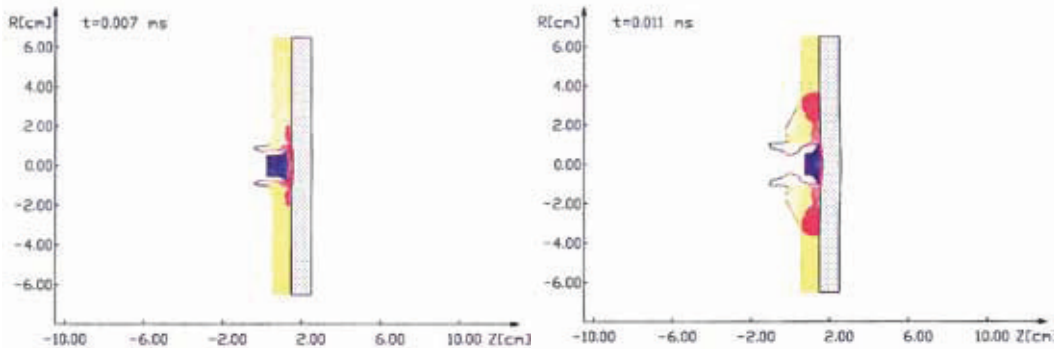

a) b)

Fig. 30. Reaction of ERA cassette: a) of 4 mm thickness explosive layer, containing 97,5% phlegmatizing agent; b) 6 mm thickness interlayer and internal radius 20 mm - 93% phlegmatizing agent, to impact of KE projectile with the speed of $V_{AP} = 1600$ [m s^{-1}]

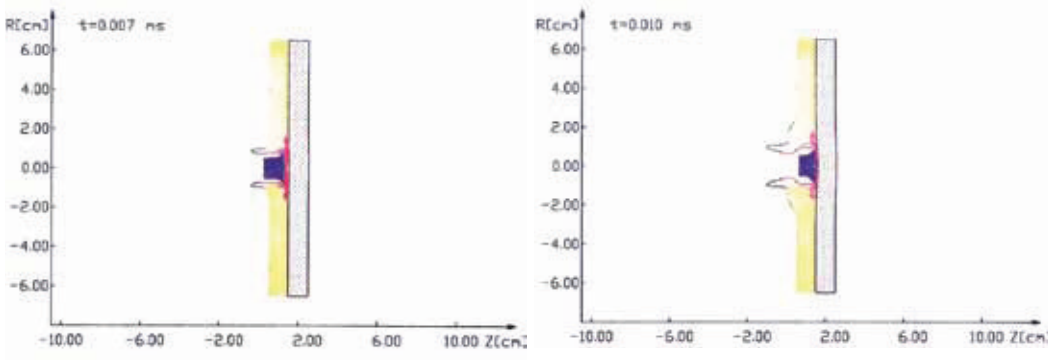

a) b)

Fig. 31. Reaction of ERA cassette: a) of 4 mm thickness explosive layer, containing 97,5% phlegmatizing agent; b) 6 mm thickness interlayer and internal radius 20 mm - 94% phlegmatizing agent, to impact of KE projectile with the speed of V_{AP} = 1600 [m s^{-1}]

4. Conclusions

4.1 In Military Institute of Armament Technology in Zielonka three generations of reactive cassettes for tank PT-91 "Hard" - ERAWA-1 and ERAWA-2 with module and block way of assembly were designed and next they were implemented in" Bumar-Łabędy" Plant and one of the examples of the third generation is presented. It can be stated that:

4.2. Cassettes are insensitive (it means that they do not detonate) after firing from small-calibre weapon, after hitting with hand grenades and mortar fragments, in result of burning petrol, napalm, incendiary agents, producing temperatures about 3000 °C on them.

4.3. Computer analysis of parameters' changes on the projectile penetration axis into ERA cassette, i.e. of density, thickness, pressure, impact velocity for different thicknesses of layers of this cassette as well as the projectile type and velocity, enables to know the initiation conditions of this cassette's explosive.

4.4. The use of computer simulation enables to know the influence of quantity of phlegmatizing agent on the sensitivity of different thicknesses explosive of one-layered and two- layered reactive cassettes.

4.5. These cassettes can be used on the other kinds of tanks and armour vehicles.

References

[1] Ogorkiewicz R.M., *Technology of tanks.* Jane's Information Group, At. K., 1991.

[2] Wiśniewski A., Zbrzeźniak R., *Segment active armour*. Patent - Poland, No 156463, 1991.

[3] Wiśniewski A., *Tank with reactive armour*. Patent - Poland, No 168122, 1992.

[4] Foss C. F., *Polish Explosive Reactive Armour Jane's Armour and Artillery 1995, 1996*, Jane' s Information Group Limited, 1995.

[5] Wiśniewski A., *Armours - Construction, Designing and Research.* Scientific and Technical Publishing House, Warsaw, 2001, (in Polish).

[6] Wiśniewski A., Żurowski W., *Ammunition and Armours.* Radom University of Technology, Radom, 2001, (in Polish).